



Published in final edited form as:

J Membr Biol. 2011 October ; 243(1-3): 47–58. doi:10.1007/s00232-011-9392-4.

Effects of Lipid-Analog Detergent Solubilization on the Functionality and Lipidic Cubic Phase Mobility of the *Torpedo californica* Nicotinic Acetylcholine Receptor

Luis F. Padilla-Morales,

Department of Chemistry, University of Puerto Rico, Río Piedras Campus, San Juan, PR 00931, USA

Claudio L. Morales-Pérez,

Department of Biology, University of Puerto Rico, Río Piedras Campus, San Juan, PR 00931, USA

Pamela C. De La Cruz-Rivera,

Department of Chemistry, University of Puerto Rico, Río Piedras Campus, San Juan, PR 00931, USA

Guillermo Asmar-Rovira,

Department of Molecular Biology, The Scripps Research Institute, La Jolla, CA, USA

Carlos A. Báez-Pagán,

Department of Biology, University of Puerto Rico, Río Piedras Campus, San Juan, PR 00931, USA

Orestes Quesada, and

Department of Physical Sciences, University of Puerto Rico, Río Piedras Campus, San Juan, PR 00931, USA

José A. Lasalde-Dominicci

Department of Biology, University of Puerto Rico, Río Piedras Campus, San Juan, PR 00931, USA,

Orestes Quesada: quesada.orestes@gmail.com; José A. Lasalde-Dominicci: jlasalde@gmail.com

Abstract

Over the past three decades, the *Torpedo californica* nicotinic acetylcholine receptor (nAChR) has been one of the most extensively studied membrane protein systems. However, the effects of detergent solubilization on nAChR stability and function are poorly understood. The use of lipid-analog detergents for nAChR solubilization has been shown to preserve receptor stability and functionality. The present study used lipid-analog detergents from phospholipid-analog and cholesterol-analog detergent families for solubilization and affinity purification of the receptor and probed nAChR ion channel function using planar lipid bilayers (PLBs) and stability using analytical size exclusion chromatography (A-SEC) in the detergent-solubilized state. We also examined receptor mobility on the lipidic cubic phase (LCP) by measuring the nAChR mobile fraction and diffusion coefficient through fluorescence recovery after photobleaching (FRAP) experiments using lipid-analog and non-lipid-analog detergents. Our results show that it is

possible to isolate stable and functional nAChRs using lipid-analog detergents, with characteristic ion channel currents in PLBs and minimal aggregation as observed in A-SEC. Furthermore, fractional mobility and diffusion coefficient values observed in FRAP experiments were similar to the values observed for these parameters in the recently LCP-crystallized β_2 -adrenergic receptor. The overall results show that phospholipid-analog detergents with 16 carbon acyl-chains support nAChR stability, functionality and LCP mobility.

Keywords

Detergent; nAChR; Lipidic cubic phase; FRAP; Fluorescence recovery; Planar lipid bilayer

Introduction

The nicotinic acetylcholine receptors (nAChRs) are the most extensively studied members of the ligand-gated ion channel (LGIC) membrane protein family. The two major nAChR subtypes are classified based on subunit composition: neuronal, composed of homopentamers or heteropentamers of subunits α_{2-10} and β_{2-4} , and both muscle and *Torpedo californica*, which are heteropentamers of subunits α , β , γ or ϵ and δ . Multiple studies have elucidated nAChR topology using site-directed mutagenesis experiments combined with electrophysiological assays (Santiago et al. 2004) and fluorescent probes to label lipid-exposed residues (Leite et al. 2003). These studies have established the overall topology of the protein: (1) a large N-terminal extracellular domain (~230 residues), (2) four putative membrane-spanning regions (TM1–TM4), (3) a large intracellular loop between TM3 and TM4 (~150 residues) and (4) a short C-terminal extracellular domain. Residues within the extracellular N-terminal form the agonist binding sites (Cymes et al. 2002; Grosman et al. 2000; Lester 2004). Amino acid residues within TM1 and especially TM2 line the ion channel pore (Langosch et al. 1988); TM3 and TM4 are predicted to be lipid-exposed and interact with nAChR annular lipids (Guzman et al. 2003; Santiago et al. 2004).

The nAChRs partly regulate cation traffic in cells and have also been implicated in several neurodegenerative diseases, such as Alzheimer disease (DeMichele-Sweet and Sweet 2010) and Parkinson disease (Quik et al. 2009), as well as brain pathologies (Gahring et al. 2005), nicotine addiction (Govind et al. 2009), inflammation (de Jonge and Ulloa 2007) and cardiovascular disease (McArdle et al. 2008). As a result of their role in all of these diseases, nAChRs represent an important target for future pharmacological therapies, not only for their direct modulation but also for the possible implications of these therapies for other LGIC protein family-related diseases. The general strategy for therapeutically targeting any protein is to identify a specific inhibitor, generally a small molecule, to block the active site or modulate the protein function through a nondirect active site interaction. This strategy often requires detailed atomic-resolution structural data that, for large protein complexes like the nAChR, can be obtained only by X-ray crystallography.

During the past three decades, great efforts have been focused on obtaining a high-resolution nAChR structure using X-ray crystallography and electron microscopy (EM). The majority of nAChR data available today come from studies using membranes and detergent-solubilized receptors obtained from the electric organs of several species of rays and eels. However, recent breakthroughs in obtaining high-resolution nAChR structural data have used heterologous expression systems such as bacteria and yeast to produce related proteins and truncated versions of the nAChR expressing only the extracellular domain. In 2001, a high-resolution crystal structure of the homologous AChBP (acetylcholine binding protein) expressed in bacteria, which has ~24% sequence identity with the nAChR and shows the same pentameric symmetry, was determined to 3.3 Å resolution (Corringer et al. 2010). In

2007, the high-resolution X-ray structure of the mouse- α_1 nAChR extracellular domain expressed in yeast was solved to 1.94 Å resolution (Dellisanti et al. 2007), providing detailed insight into the nAChR binding site and demonstrating the fundamental role of glycosylations in the binding of the α -bungarotoxin (α -BTX) antagonist.

Although the recent breakthroughs in nAChR structural data have yielded valuable insights into the soluble, ligand-binding domains, high-resolution structural data that would provide insights into the structural features of the trans-membrane domains have remained elusive. Most of the efforts at obtaining a high-resolution structure of the full-length nAChR in the detergent-solubilized state have yielded crystals, but no high-resolution X-ray data have been published (Hertling-Jaweed et al. 1988). EM studies using nAChR-enriched membranes from the electric organ of *Torpedo marmorata* led to a complete three-dimensional structure at 4.0 Å resolution (Miyazawa et al. 2003; Unwin 2005), which yielded limited structural insights as a result of the comparatively low relative atomic resolution. Recently, two independent research groups have focused on the crystallization of homologous proteins, namely bacterial LGICs. The structure of one of these prokaryotic pentameric LGICs has a topology and features similar to the nAChR (Bocquet et al. 2009; Hilf and Dutzler 2008); however, these channels have limited sequence identity, and several important features differ from those of the nAChR, such as the lack of eukaryotic posttranslational modifications that have been shown to be important to nAChR antagonist binding (Dellisanti et al. 2007). Although significant progress has been made, especially over the past decade, in obtaining high-resolution structural data for potential drug development targeting nAChR and/or LGIC family members, significant challenges remain in this regard, specifically obtaining this type of data for the transmembrane domains.

The use and choice of detergents for membrane protein studies is a key variable that may ultimately determine the success or failure of these experiments. Although many new detergents are currently available for membrane protein isolation, their behavior in solution and in the presence of the protein may limit their use with specific experimental techniques. Hence, the detergent selection and experimental conditions will have an enormous impact on whether a technique can be successfully applied to a specific membrane protein. Therefore, a clear understanding of basic detergent behavior, micelle structure and protein–detergent complexes is crucial. The study by Asmar-Rovira et al. (2008) showed how the combination of these variables influence nAChR stability and function in the detergent-solubilized state. Detergent solubilization and ligand-affinity purification of the nAChR using lipid-analog detergents—n-dodecylphosphocholine (FC-12), 3-[(3-cholamidopropyl)-dimethylammonio]-1-propane sulfonate (CHAPS) and 3 α ,7 α ,12 α -trihydroxy-5 β -cholan-24-oic acid (cholate)—resulted in a stable and functional nAChR despite significant lipid depletion, whereas the use of non-lipid-analog detergents—6-cyclohexyl-1-hexyl- β -D-malto-side (cymal-6), n-dodecyl- β -D-maltopyranoside (DDM), lauryldimethylamine-N-oxide (LDAO) and n-octyl- β -D-glucopyranoside (OG)—using the same protocols also caused significant lipid depletion, accompanied by significant aggregation and loss of ion channel function. These results highlighted not only the importance of detergent selection for membrane protein studies in the solubilized state but also the fundamental role of lipids, which have potential effects on nAChR stability and could also be a crucial criterion for the success of membrane protein structural studies. Currently, several studies on nAChR labeling and functionality have identified cholesterol, as well as anionic and neutral phospholipids, as critical for nAChR function and stability (Hamouda et al. 2006; Méthot and Baezinger 1998).

In recent years, the lipidic cubic phase (LCP) membrane protein crystallization methodology has consistently proven its viability as an alternative approach to conventional vapor diffusion by virtue of an experimental matrix that mimics the membrane protein's native

environment, making it an excellent strategy for crystallization. This in meso crystallization technique, initially presented by Landau and Rosenbusch in 1996, utilizes a bicontinuous cubic phase composed of mono-olein, water and the membrane protein of interest. The matrix consists of two compartments, a membrane system with an infinite three-dimensional periodic minimal surface interpenetrated by a system of continuous aqueous channels. Currently, there are a total 53 structures of nine different membrane proteins in the Protein Data Bank attributed to the in meso crystallization technique. During the past 4 years, LCP crystallization trials have yielded several high-resolution crystal structures of G protein-coupled receptors: β_2 -adrenergic receptor (Cherezov et al. 2007), adenosine A_{2A} receptor (Jaakola et al. 2008), CXCR4 receptor (Wu et al. 2010) and dopamine D₃ receptor (Chien et al. 2010), all of which play important roles in cardiovascular diseases, respiratory diseases and HIV infection. EM studies showed that nAChR insertion into the LCP yielded microcrystals of an nAChR- α -BTX complex that did not diffract X-rays, possibly because of size and thickness constraints (Paas et al. 2003). Loading of the nAChR- α -BTX complex on the LCP is largely affected by the physical properties of the nAChR native lipids (Paas et al. 2003) because the presence of the lipids could compromise LCP and/or protein stability and, thus, protein insertion into the matrix. For example, 1,2-dioleoyl-*sn*-glycero-3-phosphocholine (DOPC) inhibits crystal growth of the β_2 -adrenergic receptor-T4 lysozyme (β_2 AR-T4L), but cholesterol stabilizes the protein on the LCP and enhances crystal development (Liu et al. 2010). Such results suggest that lipid-protein interactions and lipid composition are critical in the examination of protein and LCP stability.

In this work, we expanded our initial approach by studying the detergent-lipid-protein stability criteria with potential lipid composition effects on the LCP in order to probe nAChR solubilization conditions that retain function and stability while showing diffusion in the LCP matrix. We used phospholipid-analog and cholesterol-analog detergent families to assay protein functionality using planar lipid bilayer (PLB) techniques and stability using analytical size exclusion chromatography (A-SEC) through estimation of the monomer, dimer and aggregate composition of the nAChR in each detergent (Asmar-Rovira et al. 2008). The nAChR stability in the LCP matrix was examined for each detergent family by measuring the mobile fraction and the diffusion coefficient of the α -BTX-nAChR complex by means of fluorescence recovery after photobleaching (FRAP). As a result, some phospholipid-and cholesterol-analog detergents were identified as candidates for further biophysical and structural studies. The overall results showed that phospholipid-analog detergents are better suited to nAChR solubilization with a minimal decrease in channel function and maintenance of nAChR stability in LCP. The combination of the techniques used in this work broadens previous efforts toward crystallization of the nAChR in its functional state.

Methods

Crude Membrane Isolation, Detergent Solubilization and Receptor Purification

Crude membrane isolation, detergent solubilization and receptor purification were carried out as described in Asmar-Rovira et al. (2008). This study examined the ion channel function and LCP mobility of the affinity-purified *T. californica* nAChR for each of the following detergents: FC-12, n-tetradecylphosphocholine (FC-14), n-hexadecylphosphocholine (FC-16) and 1-palmitoyl-2-hydroxy-*sn*-glycero-3-phosphocholine (LFC-16), from the phospholipid-analog or FC family, as well as CHAPS, 3-[(3-cholamidopropyl) dimethylammonio]-2-hydroxy-1-propanesulfonate (CHAPSO) and (*N,N'*-bis-[3-D-gluconamidopropyl] cholamide) (Big CHAP) from the cholesterol-analog family. Also, the non-lipid-analog detergents cymal-6, DDM, LDAO and OG were assayed. All detergents were obtained from Anatrace (Maumee, OH).

Sample Preparation for A-SEC

Sample preparation for A-SEC was carried out as described in Asmar-Rovira et al. (2008).

Sample Preparation, Analysis and Data Processing for PLB Assays

Sample preparation for PLB and experimental baseline were established independently for each protein–detergent complex reconstituted in the PLB and carried out as described in Asmar-Rovira et al. (2008).

Sample Preparation for LCP-FRAP, Data Collection and Analysis

FRAP experiments were performed according to the conditions and protocols described by Cherezov et al. (2008), with the following modifications: 50 μ l of a solution containing 2.0 mg/ml of ligand-affinity purified nAChR was incubated with α -BTX conjugated with Alexa-488 (Invitrogen, Carlsbad, CA) in a 1:2.5 ratio for 1.5–2 h in the dark at 4°C. The nAChR– α -BTX complex was mixed with molten mono-olein (1-oleoyl-*rac*-glycerol; Sigma-Aldrich, St. Louis, MO) in a 2:3 volume ratio, using a syringe lipid mixer, and mixed until clear appearance was observed. The nAChR– α -BTX in LCP was placed on a 75 \times 25-mm slide and washed with 1.5 ml of detergent buffer (DB-1X) solution three times before recovering the LCP-nAChR with a syringe. The LCP-nAChR was transferred into an automatic sampler, and \sim 0.2 μ l of LCP-nAChR was dispensed into 7-mm-diameter wells formed by punching holes into 50- μ m-thick transfer tape (9482PC; 3M, Minneapolis, MN) and pressing onto a glass slide. Wells were then covered by pressing a coverslip against the slide and flattening with a rubber roll (Caffrey and Cherezov 2009). This procedure was performed quickly to form a tight seal; otherwise, the LCP could dry out and compromise matrix integrity. The entire experimental procedure was performed in an environment with a relative humidity range of 60–80%. Fluorescence from unbound α -BTX could possibly interfere with the mobility studies of the affinity-purified nAChR. To rule this out, 3 μ l of a 1.0 mg/ml α -BTX-PBS solution was diluted with 100 μ l of detergent buffer, and 50 μ l of this α -BTX-detergent solution was used to perform LCP with the lipid mono-olein. After coupling each syringe with the mixer, one containing the α BTX-detergent solution and the other containing mono-olein, the sample was mixed until clear in appearance. After the cubic phase formation, the medium was washed three times with 1.5 ml of detergent buffer, recovered with a syringe, transferred onto a 75 \times 25-mm glass slide and covered with a 25 \times 25-mm coverslip, which was tightly pressed and sealed to prevent loss of moisture.

Data collection for FRAP assays was performed at room temperature using a Zeiss (Thornwood, NY) LSM 510 confocal microscope with an objective of \times 40. Five pre-bleach images were used to establish baseline fluorescence, and the laser was triggered to bleach at 75% power, immediately followed by a sequence of 500 images scanning at 2.6% power with a 0.6-s laser scanning delay. All images were obtained and processed using the Zeiss ZEN software. For data analysis each sample was integrated within a 14.0- μ m-diameter circular region of interest (ROI₁). Averaged integrated intensity of another 14.0- μ m circular region of interest (ROI₂), positioned near the bleached ROI₁, was used to correct for photobleaching from irradiation during the image-acquisition sequence. Fluorescence intensity was corrected by dividing the value of the integrated intensity ROI₁ in the bleached spot by the average integrated intensity of the ROI₂. As described by Cherezov et al. (2008), fractional fluorescence recovery curves, $F(t)$, were calculated using Eq. 1:

$$F(t)=[(f_{(t)}-f_0)/(f_{\infty}-f_0)] \quad (1)$$

where $f_{(t)}$ is the corrected fluorescence intensity of the bleached spot, f_0 is the corrected fluorescence intensity of the bleached spot in the 0.6 s after bleaching and f_{∞} is the average of corrected fluorescence intensity in the five prebleached images. Mobile fraction values

were obtained by calculating the average of the last 50 $F(t)$ values. The fractional fluorescence recovery curves were fitted with a one-dimensional exponential plot (Eq. 2), where A_i is the amplitude of each component, k is a constant related to the degree of bleaching, t is time and B is a constant related to the nAChR mobile fraction of receptors (Axelrod et al. 1976).

$$F(t) = \sum_{i=1}^n A_i (1 - e^{-kt}) + B \quad (2)$$

The diffusion coefficient value, D , was calculated using equation 3, as described by Axelrod et al. (1976) and Pucadyil and Chattopadhyay (2006), where γ is a constant that corresponds to a circular beam shape, R is the beam radius and $t_{1/2}$ equals $\ln 2/k$, where k is obtained from the fitting of $F(t)$.

$$D = [(\gamma R^2) / (4t_{1/2})] \quad (3)$$

Results

PLB Characterization of Affinity-Purified nAChR Using Phospholipid-Analog Detergents

All nAChR purifications with phospholipid-analog detergents retained ion channel function, with well-defined opening–closing signals (Fig. 1) that were similar to those observed in previous studies with phospholipid-analog detergents (Asmar-Rovira et al. 2008). Although the three phospholipid-analog detergents used in this study (FC-12, FC-14, FC-16) have the same head group and differ only by two or four methyl groups in their hydrophobic tails, remarkable differences were observed in ion channel traces and mean single-channel current values (Fig. 1a–d). The overall results suggest a correlation between the average current values for the detergent and the hydrophobic chain length. Despite the fact that LFC-16 shares the same head group with all of the previously mentioned phospholipid analogs and that it is a lysophospholipid of phosphatidylcholine instead of a phosphate ether (Table 1), it shows similar mean ion channel currents to those of FC-16.

PLB Characterization of Affinity-Purified nAChR Using Cholesterol-Analog Detergents

CHAPS and CHAPSO are zwitterionic detergents and sulfobetaine derivatives of cholic acid with almost identical structures, whereas cholate is negatively charged with a carboxylic acid tail. Affinity-purified nAChR using these cholesterol-analog detergents retains ion channel function, and they have similar ion channel traces; mean ion channel current values were CHAPS -1.44 ± 0.01 pA and CHA-PSO -1.92 ± 0.04 pA (Fig. 2).

A-SEC Assays for Affinity-Purified nAChR

Affinity-purified nAChR in each detergent at a concentration of 1–5 mg/ml was subjected to A-SEC after incubation with α -BTX–Alexa-488 as described previously (Asmar-Rovira et al. 2008). The fluorescence intensities of each peak corresponding to the monomer, dimer, aggregate and free α -BTX–Alexa 488 were recorded for each detergent. The nAChR stability in each detergent was probed by comparing the amount of aggregation in detergent solution. Both cholesterol- and phospholipid-analog detergents showed some degree of aggregation in A-SEC, implying nAChR unfolding and degradation in both detergent subtypes. However, the degree of stability was considerably higher for cholesterol analogs than for phospholipid analogs, suggesting that phospholipid-analog detergents are more

suitable than cholesterol-analog detergents at preserving nAChR stability in the detergent-solubilized state (Figs. 1, 2).

FRAP of Affinity-Purified *T. californica* nAChR in LCP: Validation of Experimental Data

Fluorescence recovery experiments were visualized using the fluorescence signal from α -BTX–Alexa-488 bound to nAChR. First, we evaluated whether unbound α -BTX could interfere with mobility studies of the affinity-purified nAChR– α -BTX complex. A simple experiment showed that incorporation of free α -BTX can be controlled by washing the already prepared nAChR-LCP three times with detergent buffer, as described in Methods. To identify fluorescent traces of free α -BTX, the LCP was irradiated with a 488-nm argon laser at 5% power and scanning was performed manually at a 500–550 nm range using a $\times 40$ lens for any sign of fluorescent light sources. The observed fluorescence arose from the region surrounding the LCP matrix, indicating that the α -BTX was partitioned into the water interface surrounding the LCP and, thus, was completely excluded from it (Fig. 3a, b). α -BTX binding was unaffected by the identity of the detergents used since we were able to complex the nAChR to α -BTX–Alexa-488 in A-SEC stability assays.

Effects of Phospholipid-Analog Detergents on LCP Mobility and Diffusion

Figure 4 presents the fractional fluorescence recovery data for affinity-purified *T. californica* nAChR in phospholipid-analog detergents labeled with α -BTX and in the LCP matrix, fitted with a single component diffusion equation (Eq. 2). As described in Methods, two 14.0- μm ROI circular areas were used for FRAP experiments, where fluorescence intensities were monitored at 0.6-s intervals. Considerable differences in the initial rate of the fluorescence recovery curves were observed within the first 100 s, suggesting that a combination of factors besides the hydrophobic tail and head group of the detergents in the protein–detergent complex influenced nAChR diffusion. In general terms, a higher percentage of nAChR in the monomeric state yielded a higher mobile fraction in LCP-FRAP. Solubilization and purification of the nAChR using LFC-16 produced $\sim 82\%$ monomeric composition and a high mobile fraction of $\sim 85\%$; FC-16 produced $\sim 74\%$ monomeric composition and an $\sim 87\%$ mobile fraction (Fig. 4a). These mobile fractions are similar to those reported as crystallization conditions of the β_2 -adrenergic receptor–T4L in LCP (Cherezov et al. 2008). These results indicate that the percentage of monomer in the nAChR sample positively affects the receptor mobile fraction in the LCP matrix. Diffusion coefficient differences are negligible among all detergents except for LFC-16, which shows an order of magnitude faster diffusion than the others, perhaps due to a potentially significant combination of the unique hydrophobic tail linker and the percentage of nAChR monomer for LFC-16, as described previously (Fig. 4b). Interestingly, FC-16 reaches the plateau much slower than the other detergents but eventually achieves the same maxima as LFC-16. In conclusion, there is an apparent correlation between chain length, A-SEC monomer percentages and mobile fraction, with longer chain lengths and higher A-SEC monomer percentages corresponding to higher mobile fractions.

Effects of Cholesterol-Analog Detergents on LCP Mobility and Diffusion

Similar to findings with the phospholipid-analog detergents, FRAP data from cholesterol analogs fit very well with a single component diffusion equation (Fig. 5). Overall, no substantial differences in the diffusion coefficients were observed for cholesterol-analog detergents: all of them showed similar diffusion coefficients of $\sim 7.50 \times 10^{-9} \text{ cm}^2/\text{s}$, except for CHAPS, which produced a higher diffusion coefficient of $1.92 \times 10^{-8} \text{ cm}^2/\text{s}$ (Fig. 5b). CHAPS and cholate yielded nAChR mobile fractions of 71% and 89%, respectively, while Big CHAP showed a mobile fraction of 37%. FRAP of crude *T. californica* membranes showed $\sim 10\%$ mobile fraction. No correlation was apparent between monomer percentages and diffusion coefficients and/or different structural features of the cholesterol analogs

themselves. However, in our previous study (Asmar-Rovira et al. 2008) the cholesterol-analog detergents CHAPS and cholate showed negligible amounts of residual native lipid and high purity (SDS-PAGE) following ligand-affinity purification, whereas Big CHAP showed significant amounts of residual native lipid and noticeable background contaminants in SDS-PAGE. These observations suggest that the significant reduction in mobile fraction observed for Big CHAP compared to other cholesterol-analog detergents could be due to the residual native lipid and/or contaminant proteins, which would be supported by the minimal diffusion observed for the crude membrane fraction.

Effects of Non-Lipid-Analog Detergents on LCP Mobility and Diffusion

Asmar-Rovira et al. (2008) previously established that some non-lipid-analog detergents, such as cymal-6, DDM, LDAO and OG, used to obtain affinity-purified nAChR from *T. californica* membranes yield a nonfunctional receptor. However, FRAP data of affinity-purified nAChR in these detergents fit well in a single component diffusion curve, with no substantial differences observed when comparing the mobile fraction and diffusion coefficients for these detergents. Diffusion coefficients for LDAO, DDM and OG determined from Eq. 3 (see “Methods” section) were 9.88×10^{-9} , 1.99×10^{-8} and 1.34×10^{-8} cm²/s, respectively. These results indicate that a nonfunctional receptor in non-lipid-analog detergents diffuses as well as receptor solubilized using lipid-analog detergents in the LCP matrix (Fig. 6).

Discussion and Conclusions

The PLB assay for the affinity-purified *T. californica* nAChR in phospholipid and cholesterol analogs showed no considerable difference in single-channel mean current under the same voltage-clamp conditions, even for members of the same detergent family, as previously reported (Asmar-Rovira et al. 2008). Differences in the mean channel current between our former study (Asmar-Rovira et al. 2008) and this current work (1.25 pA) are attributed first to variability between the tissue sources and largely to differences in the membrane resistance and capacitance. During the PLB assay, both plastic holder cavities were filled with the same bilayer buffer solution; however, the final concentration in the front plastic holder was slightly different due to necessary additional components (see “Methods” section). This will modify the ion concentration in both chambers with the concomitant alteration of electromotive force that could generate differences between sample preparations.

Lipid depletion, which is an inevitable consequence of the protein membrane solubilization process, could be responsible for the aggregation and monomer–dimer ratios that affect ion channel function. If we consider the nAChR monomer, dimer and aggregate percentages for each of the detergents used in this study obtained using A-SEC and compare them with the total mobile fraction in FRAP assays, a discrepancy in the mobile fraction is apparent. The monomer should be the species that displays the greatest mobility in the LCP matrix; therefore, the mobile fraction values for the cholesterol-analog detergents CHAPS, CHAPSO, Big CHAP and cholate should be minimal. However, their mobile fraction values of 71%, 81%, 49% and 87%, respectively, are much higher than expected, with similar results observed for other lipid-analog and non-lipid-analog detergents. Furthermore, phospholipid-analog detergents also showed a higher than expected mobile fraction based on the contribution of the monomers observed in the A-SEC assays. In the case of LFC-16, a direct correlation was observed between the amount of monomer detected on A-SEC and the FRAP mobile fraction. Bearing in mind that the protein–detergent complex needs to be mixed with the matrix of the LCP to maximize the intermolecular interactions with mono-olein, it is not surprising that those detergents that contain hydrophobic regions, consisting mainly of aliphatic chains, can form better stabilizing interactions with the mono-olein

structure. These interactions can be the driving force necessary to filter the dimers and aggregates of the protein and facilitate its incorporation into the LCP matrix. The cholesterol- and lipid-analog detergents that were chosen for these studies contain moieties in their structure that enable them to interact with the 16-carbon chain of mono-olein. Theoretically, the best interaction should be produced by the 16-carbon lysophosphatidylcholine, which was the detergent that produced an affinity-purified nAChR with the most monomeric species and stable crystals in a 30-day study period (supplementary Fig. S2).

The use of FRAP in protein reconstituted in LCP as a precrystallization assay to select suitable conditions for in meso crystallization of membrane protein complemented with PLB studies could be a powerful strategy for future nAChR X-ray crystallographic studies. FRAP measurements in LCP were performed using the α -BTX–Alexa-488 nAChR antagonist to label the affinity-purified nAChR in different detergents. Also, our FRAP results rule out the possibility that the LCP matrix could not hold the nAChR due to its size, a molecular weight of approximately 290 kDa (Unwin 2005). However, our results clearly indicated that the LCP matrix could incorporate the nAChR complex because all of the samples assayed showed an adequate mobile fraction. Therefore, it would not be necessary to use a system such as the sponge phase that would provide a greater curvature, which is necessary for the incorporation of large proteins.

The FRAP curves for nAChR– α -BTX–Alexa-488 complex in LCP following affinity purification for lipid-analog detergents in Fig. 4 showed fractional fluorescence recovery ranging 60–87%, with a fast phase of approximately 150 s followed by a slower phase. Data were collected every 0.6 s for the entire experimental period of 500 s. Maximum recoveries were established near the 300-s mark, where FC-16 and LFC-16 were found to have approximately the same value. However, the rate of recovery was different for all lipid-analog detergents assayed, with LFC-16 being the one that showed the highest rate of recovery. The diffusion constant obtained from Eq. 3 for each of the phosphocholine ethers showed a decrease proportional to the length of the acyl carbon chain. This trend suggests possible stabilization of the protein–detergent complexes, while the acyl chain of the detergent increases to the same length of the acyl chain of the mono-olein that composes the LCP matrix. At first glance, this correlation appears to be inappropriate because LFC-16 and FC-16 have the same length in the acyl chain. LFC-16 has an *sn*-1-acyl glycerol backbone esterified to a phosphocholine head group. However, the LFC-16 head group can adopt a different conformation angle in relation to the bilayer plane and has the possibility of establishing ionic interactions with amino acids embedded in the nAChR water–lipid interface, which would not be accessible to other ether analogs, increasing nAChR solubility in the LCP matrix. Our FRAP results of nAChR-enriched crude membranes in Figs. 4, 5, 6 indicate limited diffusion capacity, which is not surprising since the crude membrane has a significant amount of other integral and membrane-associated proteins that would limit nAChR diffusion.

Figure 5 illustrates the behavior of cholesterol-analog detergents on FRAP measurements using the LCP matrix. The detergents cholate and CHAPSO have a similar fluorescence recovery rate during the initial 100 s, with slightly different maximum fractional fluorescence values. Big CHAP and CHAPS showed a difference in both the initial rate during the first 100 s and the plateau value of fractional percentage of fluorescence. The mobile fraction of Big CHAP is about half that of its counterpart cholate, which can be attributed to the polyalcohol functional groups of the head group of Big CHAP. These hydroxyl groups could potentiate hydrogen bonds with other detergent molecules, mono-olein or nAChR amino acids. These interactions could stabilize the nAChR dimers and aggregates and be responsible for the poor incorporation and slow diffusion of the receptor

in the LCP matrix. On the other hand, the negatively charged cholesterol analog cholate showed similar behavior with respect to the FRAP curves and mobile fraction. Cholate is 85% more efficient at producing nAChR monomer and dimer following affinity column purification (Asmar-Rovira et al. 2008). Zwitterionic detergents such as CHAPS and CHAPSO showed mobile fraction values of 71% and 81%, respectively. These values are similar to those obtained for the negatively charged cholate, suggesting that the head-group charge is not a determinant factor in the mobile fraction of the nAChR after affinity column purification with this family of detergents. Interestingly, throughout the cholesterol-analog series, all of them yielded low amounts of monomer according to the A-SEC results. Despite the structural differences between detergents, the mobile fraction is particularly affected by the total lipid composition of the nAChR. As previously reported, the total lipid composition of the affinity-purified nAChR for CHAPS is 45 nmol; for cholate, 47 nmol; and for Big CHAP, 143 nmol (Asmar-Rovira et al. 2008).

Figure 6 shows two different detergents that contain 8- and 12-carbon aliphatic chains, respectively: OG with a glucopyranoside head group (mobile fraction 76%) and DDM with a maltose head group (mobile fraction 74%). The initial rate of fluorescence recovery during the first 100 s for these detergents is very similar. Figure 6 also shows data for LDAO, a 12-alkyl dimethylamine oxide detergent, which yielded a mobile fraction of 83% with an nAChR monomer population of ~28% in A-SEC, which is very similar to that of DDM. With the exception of OG, which shows a total depletion of the monomer species upon affinity purification in A-SEC, all of these non-lipid-analog detergents have a similar 1:2–1:3 monomer–dimer ratio following purification. In that sense, they show a similar trend to cholesterol-analog detergents, which showed similar monomer–dimer ratios upon affinity purification. In fact, when one compares the FRAP assays for LFC-16, CHAPS, DDM and OG, they reflect identical diffusion coefficients that are ~10 times faster than the other detergents. These results suggest that, despite the aggregation observed in A-SEC and loss of ion channel function in bilayer assays observed for non-lipid-analog detergents, these detergents are capable of diffusion rates on LCP-FRAP that are comparable to some of the rates observed for lipid-analog detergents (Asmar-Rovira et al. 2008).

This study presents the first FRAP quantitative measurements for the nAChR in LCP, providing diffusion rates and mobile fractions with different phospholipid- and cholesterol-analog detergents, which can offer new guidance for further crystallization trails. Ultimately, decoding the mechanism(s) by which detergents affect the lipid composition, stability and functional state of membrane proteins may lead to the development of novel strategies that would enhance the crystallization of membrane proteins. Our study shows that there are remarkable differences in nAChR stability for phospholipid- and cholesterol-analog detergents. Phospholipid-analog detergents with 16 carbon chains are more likely to maintain reasonable nAChR function and stability. The results presented here highlight the importance of determining nAChR function in the LCP matrix since detergent–protein complexes that are nonfunctional in PLB assays yielded highly mobile fractions in LCP-FRAP, and further efforts should be directed toward this goal. Another factor to be considered is the possibility that the LCP could function as a “filter” for the inclusion of monomeric and exclusion of dimeric protein species into the LCP matrix. These results provide important information for the preparation of functionally active nAChR–detergent complexes. An implicit assumption of the results from the detergent-solubilized nAChR with respect to functionality, stability and state of aggregation of the nAChR is that they will be relevant to other important membrane receptor systems, ion channels and membrane proteins.

Supplementary Material

Refer to Web version on PubMed Central for supplementary material.

Acknowledgments

This work was supported by National Institutes of Health (NIH) grants 2RO1GM56371-12, 5T34GM07821-31, Minority Access to Research Careers (MARC) and 2R25GM061151; Research Initiative for Scientific Enhancement (RISE); University of Puerto Rico Río, Piedras Campus Institutional Funds for Research; and the Specialized Neurosciences Research Program (SNRP) U54NS0433011. We acknowledge the contribution to this study by grants 1S10RR 13705-01 and DBI-0923132 to establish and upgrade the Confocal Microscopy Facility at the University of Puerto Rico (CIF-UPR) and the University of Puerto Rico Institutional Funds. We thank Dr. Raymond Stevens for access to the A-SEC instrumentation, Dr. Vadim Cherezov for expert advice in FRAP, Dr. Hernán Martínez for his commentaries about FRAP data analysis and Manuel Delgado-Vélez for critical reading.

References

- Asmar-Rovira GA, Asseo-García AM, Quesada O, Hanson MA, Cheng A, Noguera C, Lasalde-Dominicci JA, Stevens RC. Biophysical and ion channel functional characterization of the *Torpedo californica* nicotinic acetylcholine receptor in varying detergent–lipid environments. *J Membr Biol.* 2008; 223:13–26. [PubMed: 18581036]
- Axelrod D, Koppel DE, Schlessinger J, Elson E, Webb WW. Mobility measurement by analysis of fluorescence photobleaching recovery kinetics. *Biophys J.* 1976; 16:1055–1069. [PubMed: 786399]
- Bocquet N, Nury H, Baaden M, Le Poupon C, Changeux JP, Delarue M, Corringer PJ. X-ray structure of a pentameric ligand-gated ion channel in an apparently open conformation. *Nature.* 2009; 457:111–114. [PubMed: 18987633]
- Caffrey M, Cherezov V. Crystallizing membrane proteins using lipidic mesophases. *Nat Protoc.* 2009; 4:707–731.
- Cherezov V, Rosenbaum DM, Hanson MA, Rasmussen SG, Thian FS, Kobilka TS, Choi HJ, Kuhn P, Weis V, Kobilka BK, Stevens RC. High-resolution crystal structure of an engineered human beta₂-adrenergic G protein-coupled receptor. *Science.* 2007; 318:1258–1265. [PubMed: 17962520]
- Cherezov V, Liu J, Griffith M, Hanson MH, Stevens RC. FRAP assay for pre-screening membrane proteins for in meso crystallization. *Cryst Growth Des.* 2008; 8:4307–4315.
- Chien EY, Liu W, Zhao Q, Katritch V, Han GW, Hanson MA, Shi L, Newman AH, Javitch JA, Cherezov V, Stevens RC. Structure of the human dopamine D₃ receptor in complex with a D₂/D₃ selective antagonist. *Science.* 2010; 330:1091–1095. [PubMed: 21097933]
- Corringer PJ, Baaden M, Bocquet N, Delarue M, Dufresne V, Nury H, Prevost M, Van Renterghem V. Atomic structure and dynamics of pentameric ligand-gated ion channels: new insight from bacterial homologues. *J Physiol.* 2010; 588:565–572. [PubMed: 19995852]
- Cymes GD, Grosman C, Auerbach A. Structure of the transition state of gating in the acetylcholine receptor channel pore: a phi-value analysis. *Biochemistry.* 2002; 41:5548–5555. [PubMed: 11969415]
- de Jonge WJ, Ulloa L. The alpha7 nicotinic acetylcholine receptor as a pharmacological target for inflammation. *Br J Pharmacol.* 2007; 151:915–929. [PubMed: 17502850]
- Dellisanti CD, Yao Y, Stroud JC, Wang ZZ, Chen L. Crystal structure of the extracellular domain of nAChR α_1 bound to α -bungarotoxin at 1.94 Å resolution. *Nat Neurosci.* 2007; 10:953–962. [PubMed: 17643119]
- DeMichele-Sweet MA, Sweet RA. Genetics of psychosis in Alzheimer's disease: a review. *J Alzheimers Dis.* 2010; 19:761–780. [PubMed: 20157235]
- Gahring LC, Persiyonov K, Rogers SW. Mouse strain-specific changes in nicotinic expression with age. *Neurobiol Aging.* 2005; 26:973–980. [PubMed: 15718057]
- Govind AP, Vezina P, Green WN. Nicotine-induced upregulation of nicotinic receptors: underlying mechanisms and relevance to nicotine addiction. *Biochem Pharmacol.* 2009; 78:756–765. [PubMed: 19540212]

- Grosman C, Salamone FN, Sine SM, Auerbach A. The extracellular linker of muscle acetylcholine receptor channels is a gating control element. *J Gen Physiol.* 2000; 116:327–340. [PubMed: 10962011]
- Guzman GR, Santiago J, Ricardo A, Marti-Arbona R, Rojas LV, Lasalde-Dominicci JA. Tryptophan scanning mutagenesis in the alphaM3 transmembrane domain of the *Torpedo californica* acetylcholine receptor: functional and structural implications. *Biochemistry.* 2003; 42:12243–12250. [PubMed: 14567686]
- Hamouda AK, Sanghvi M, Sauls D, Machu TK, Blanton M. Assessing the lipid requirements of the *Torpedo californica* nicotinic acetylcholine receptor. *Biochemistry.* 2006; 45:4327–4337. [PubMed: 16566607]
- Hertling-Jaweed S, Bandini G, Muller-Fahrnow A, Dommes V, Hucho F. Rapid preparation of the nicotinic acetylcholine receptor for crystallization in detergent solution. *FEBS Lett.* 1988; 241:29–32. [PubMed: 3197836]
- Hilf R, Dutzler R. X-ray structure of a prokaryotic pentameric ligand-gated ion channel. *Nature.* 2008; 452:375–379. [PubMed: 18322461]
- Jaakola VP, Griffith MT, Hanson MA, Cherezov V, Chien EY, Lane JR, Ijzerman AP, Stevens RC. The 2.6 angstrom crystal structure of a human A2A adenosine receptor bound to an antagonist. *Science.* 2008; 322:1211–1217. [PubMed: 18832607]
- Landau EM, Rosenbusch JP. Lipidic cubic phase: a novel concept for the crystallization of membrane proteins. *Proc Natl Acad Sci USA.* 1996; 93:14532–14535. [PubMed: 8962086]
- Langosch D, Thomas L, Betz H. Conserved quaternary structure of ligand-gated ion channels: the postsynaptic glycine receptor is a pentamer. *Proc Natl Acad Sci USA.* 1988; 85:7394–7398. [PubMed: 2459705]
- Leite JF, Blanton MP, Shahgholi M, Dougherty DA, Lester HA. Conformation-dependent hydrophobic photolabeling of the nicotinic receptor: electrophysiology-coordinated photochemistry and mass spectrometry. *Proc Natl Acad Sci USA.* 2003; 100:13054–13059. [PubMed: 14569028]
- Lester RA. Activation and desensitization of heteromeric neuronal nicotinic receptors: implications for non-synaptic transmission. *Bioorg Med Chem Lett.* 2004; 14:1897–1900. [PubMed: 15050622]
- Liu W, Hanson MA, Stevens RC, Cherezov V. LCP-Tm: an assay to measure and understand integrity of membrane proteins in a membrane environment. *Biophys J.* 2010; 98:1539–1548. [PubMed: 20409473]
- McArdle PF, Rutherford S, Mitchell BD, Damcott CM, Wang Y, Ramachandran V, Ott S, Chang YP, Levy D, Steinle N. Nicotinic acetylcholine receptor subunit variants are associated with blood pressure; findings in the Old Order Amish and replication in the Framingham Heart Study. *BMC Med Genet.* 2008; 9:67. [PubMed: 18625075]
- Méthot N, Baezinger JE. Secondary structure of the exchange resistance core from the nicotinic acetylcholine receptor probed directly by infrared spectroscopy and hydrogen/deuterium exchange. *Biochemistry.* 1998; 37:4815–14822. [PubMed: 9537998]
- Miyazawa A, Fujiyoshi Y, Unwin N. Structure and gating mechanism of the acetylcholine receptor pore. *Nature.* 2003; 423:949–955. [PubMed: 12827192]
- Paas Y, Cartaud J, Recouvreux M, Grailhe R, Dufresne V, Pebay-Peyroula E, Landau EM, Changeux JP. Electron microscopic evidence for nucleation and growth of 3D acetylcholine receptor microcrystals in structured lipid detergent matrices. *Proc Natl Acad Sci USA.* 2003; 100:11309–11314. [PubMed: 13679581]
- Pucadyil TJ, Chattopadhyay A. Confocal fluorescence recovery after photobleaching of green fluorescent protein in solution. *J Fluoresc.* 2006; 16:87–94. [PubMed: 16397826]
- Quik M, Huang LZ, Parameswaran N, Bordia T, Campos C, Perez XA. Multiple roles for nicotine in Parkinson's disease. *Biochem Pharmacol.* 2009; 78:677–685. [PubMed: 19433069]
- Santiago J, Guzman GR, Torruellas K, Rojas LV, Lasalde-Dominicci JA. Tryptophan scanning mutagenesis in the TM3 domain of the *Torpedo californica* acetylcholine receptor beta subunit reveals an alpha-helical structure. *Biochemistry.* 2004; 43:10064–10070. [PubMed: 15287734]
- Unwin N. Refined structure of the nicotinic acetylcholine receptor at 4 Å resolution. *J Mol Biol.* 2005; 46:967–989. [PubMed: 15701510]

Wu B, Chien EY, Mol CD, Fenalti G, Liu W, Katritch V, Abagyan R, Brooun A, Wells P, Bi FC, Hamel DJ, Kuhn P, Handel TM, Cherezov V, Stevens RC. Structures of the CXCR4 chemokine GPCR with small-molecule and cyclic peptide antagonists. *Science*. 2010; 330:1066–1071. [PubMed: 20929726]

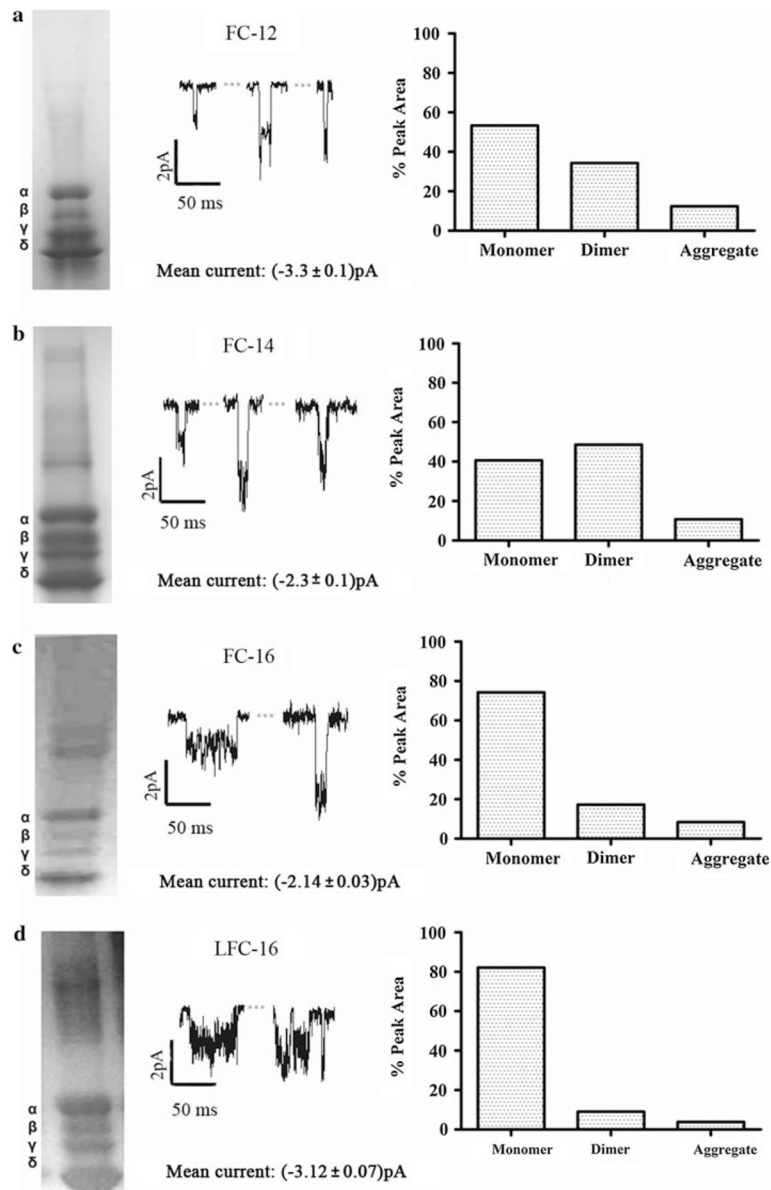


Fig. 1. Current traces of affinity-purified nAChR using phospholipid-analog detergents. PLB current traces at -70 mV membrane potential with 0.5 M of carbamylcholine chloride (*middle panel*), SDS-PAGE gels (*left panel*) and A-SEC stability assays (*right panel*) for **a** FC-12 monomer (53.3%)/dimer (34.3%)/aggregate (12.4%), **b** FC-14 monomer (40.6%)/dimer (48.6%)/aggregate (10.8%), **c** FC-16 monomer (74.3%)/dimer (17.3%)/aggregate (8.4%) and **d** LFC-16 monomer (82.1%)/dimer (9.0%)/aggregate (3.9%). For each detergent condition, an average of three independent bilayer experiments with duration of ~ 20 min each was performed

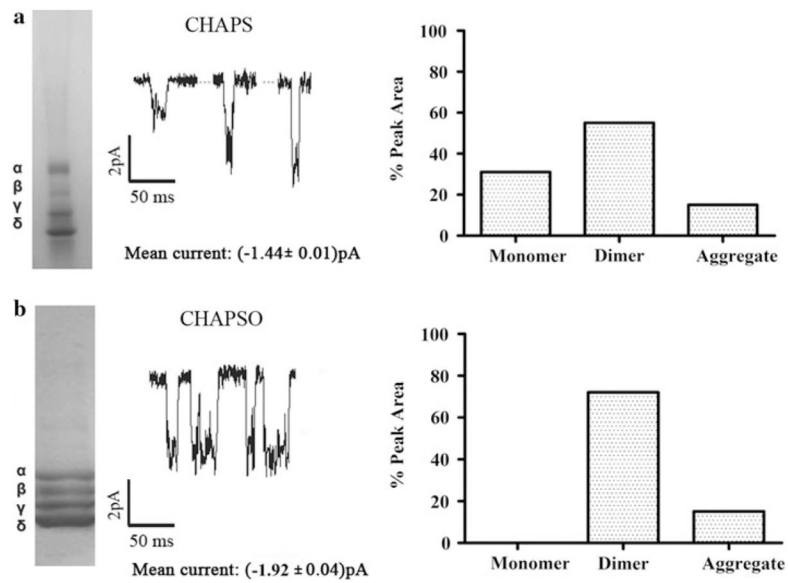


Fig. 2. Current traces of affinity-purified nAChR using cholesterol-analog detergents. PLB current traces at -70 mV membrane potential with 0.5 M of carbamylcholine chloride (*middle panel*), SDS-PAGE gels (*left panel*) and A-SEC stability assays (*right panel*) for **a** CHAPS monomer (30%)/dimer (55%)/aggregate (15%) and **b** CHAPSO monomer (0.0%)/dimer (72.7%)/aggregate (27.3%). For each detergent condition, averages of three independent bilayer experiments with duration of ~ 20 min each were performed

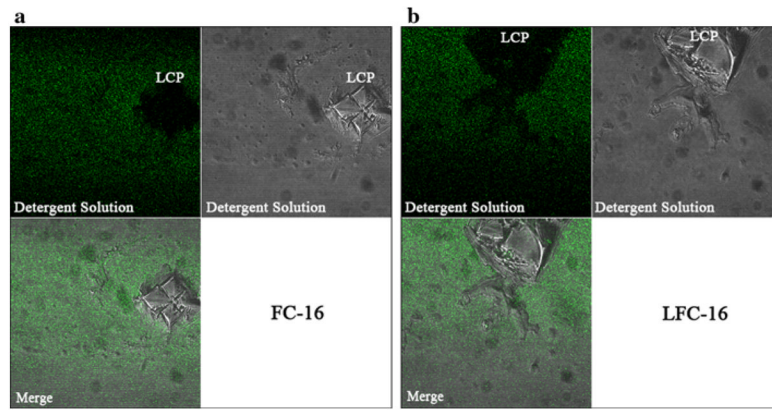


Fig. 3. FRAP control experiments show that α -BTX does not bind to or mix with the LCP matrix in the absence of nAChRs; thus, it is a nonsignificant source of background fluorescence. The protocol for α -BTX removal is described in “Methods” section

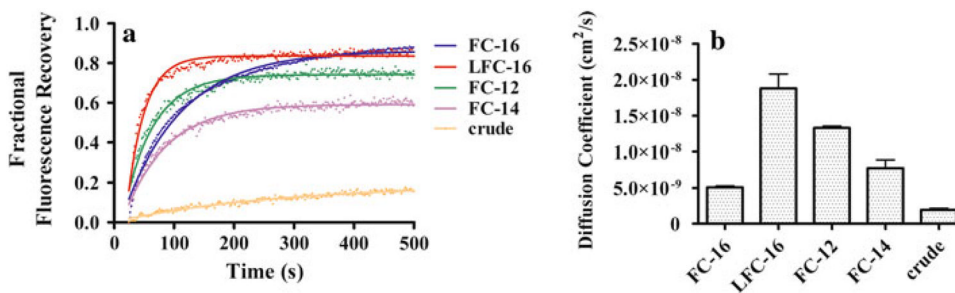


Fig. 4. Fractional fluorescence recovery and diffusion coefficient of each affinity-purified nAChR using phospholipid-analog detergents. FRAP experiments (a) were recorded for affinity-purified nAChR using the phospholipid-analog detergents FC-16, LFC-16, FC-12 and FC-14. All fluorescence recovery experiments were performed in duplicate, averaging three recoveries on different areas of the LCP with the nAChR incorporated. The fractional recovery was calculated for each phospholipid-analog detergent using Eq. 1 for each fractional fluorescence recovery of the duplicates. The diffusion coefficient (b) was calculated using Eqs. 2 and 3 for each phospholipid-analog detergent

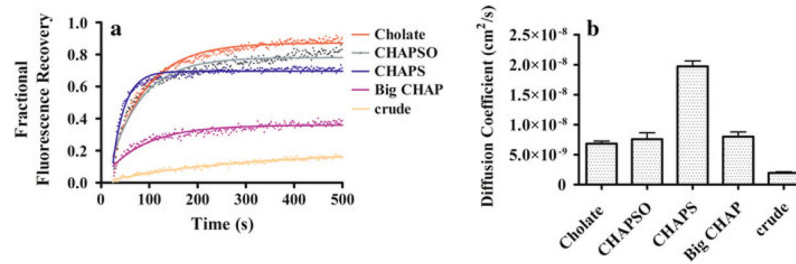


Fig. 5.

Fractional fluorescence recovery and diffusion coefficient for each affinity-purified nAChR using cholesterol-analog detergents. FRAP experiments (**a**) were recorded for affinity-purified nAChR using the cholesterol-analog detergents cholate, CHAPSO, CHAPS and Big CHAP. All fluorescence recovery experiments were performed in duplicate, averaging three recoveries on different areas of the LCP with the nAChR incorporated. The fractional recovery was calculated for each cholesterol-analog detergent using Eq. 1 for each fractional fluorescence recovery of the duplicates. The diffusion coefficients (**b**) were calculated using Eqs. 2 and 3 for each cholesterol-analog detergent

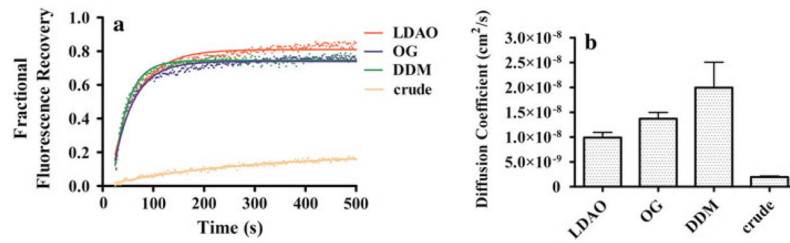
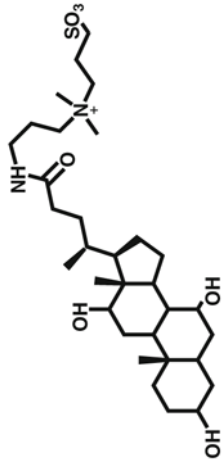
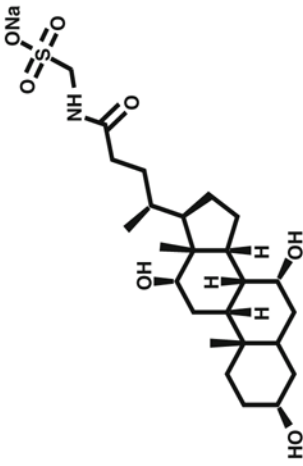


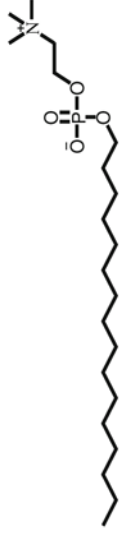


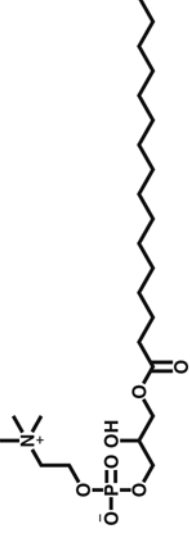
Fig. 6.

Fractional fluorescence recovery and diffusion coefficient of each affinity-purified nAChR using non-lipid-analog detergents. FRAP experiments (a) were recorded for affinity-purified nAChR using the non-lipid-analog detergents LDAO, OG and DDM. All fluorescence recovery experiments were performed in duplicate, averaging three recoveries on different areas of the LCP with the nAChR incorporated. The fractional recovery was calculated for each non-lipid-analog detergent using Eq. 1 for each fractional fluorescence recovery of the duplicates. The diffusion coefficient (b) was calculated using Eqs. 2 and 3 for each non-lipid-analog detergent

Table 1

Chemical and physical properties of the lipid-analog detergents

| Name | CMC (mM) | Aggregation number | Solubilization concentration (mM) | Affinity column wash buffer concentration (mM) | Structure |
|--------------------------------|----------|--------------------|-----------------------------------|--|---|
| Cholesterol-analog detergents | | | | | |
| CHAPS | ~8 | 10 | 32.5 (2%) | 12 |  |
| CHAPSO | ~8 | 11 | 32.5 (2%) | 12 |  |
| Phospholipid-analog detergents | | | | | |
| FC-12 | 1.5 | 54 | 28.4 (1%) | 2.25 |  |
| FC-14 | 0.12 | 108 | 26.35 (1%) | 0.18 |  |
| FC-16 | 0.013 | 178 | 24.53 (1%) | 0.20 |  |

| Name | CMC (mM) | Aggregation number | Solubilization concentration (mM) | Affinity column wash buffer concentration (mM) | Structure |
|--------|----------|--------------------|-----------------------------------|--|---|
| LFC-16 | 0.0032 | n/a | 20.17 (1%) | 0.0048 |  |